EFFECTS OF COULOMB FRICTION ON THE PERFORMANCE OF A SERVOMECHANISM HAVING BACKLASH. PART II—TRANSIENT RESPONSE CONSIDERATIONS

A. K. MAHALANOBIS

INSTITUTE OF RADIOPHYSICS AND ELECTRONICS, UNIVERSITY COLLEGE OF TECHNOLOGY, CALCUTTA

(*Received, October 9*, 1960)

ABSTRACT. The paper gives results of analysis of the effects of coulomb friction on the transient response of a servo system containing backlash in the output coupling. First, the qualitative aspects of the transient response characteristics are discussed with the help of frequency response methods; next, a quantiative discussion of the same is provided with the help of a piece-wise linear solution of the characteristic differential equations. Simulator results in support of the theoretical observations are also given.

INTRODUCTION

In a previous paper the effects of coulomb friction on the stability of sustained oscillations in a second order servomechanism having backlash in the output coupling was discussed (Mahalanabis, 1960). The coulomb friction has been taken to be present in the driving member. A describing function was developed for the motor under the action of the nonlinear friction; it was discussed how presence of coulomb friction helps to avoid sustained oscillations that are otherwise produced by the system backlash.

Beside the question of the stability of sustained oscillations the stability of the response of a system in the transient state is also of considerable interest to servo designers. In the present paper the relative stability of a servo system affected by the two nonlinearities under consideration viz. backlash and coulomb friction has been analysed.

It is to be mentioned that the discussions that follow have been based on the results of application of two methods. First, the results of application of the frequency response method are presented. These are necessarily of approximate nature but are nevertheless of interest since this is perhaps the most nearly generalised approach available at present for nonlinear systems analysis. More accurate data on the transient response of the system concerned are provided by solution of the piece-wise linear differential equations that characterise the system.

Finally, the response of a system simulated on an electronic analogue computer for step displacement inputs is presented as an experimental aid to the understanding of the system transient behaviour.

SYSTEM UNDER CONSIDERATION

The system under consideration has been described in part I (Mahalanobis, 1960) in some details and will be only briefly outlined here for the sake of convenience. The system is shown in Fig. 1 in the schematic form. Nonlinearities

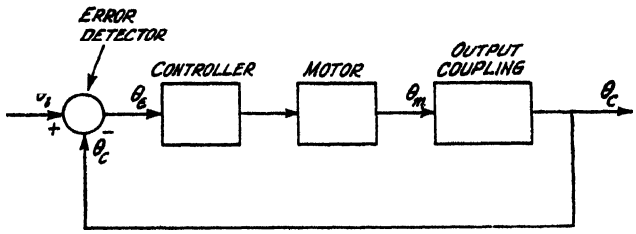

Fig. 1. System under consideration

are assumed in (i) the motor shaft whose motion is taken to be subject to both viscous and coulomb frictions and (ii) the output coupling unit which is taken to have backlash. The load is assumed to be a resistive one so that the nonlinear characteristics resulting from the coupling-unit backlash is as shown in Fig. 2. In Fig. 3 is depicted the composite friction characteristics of the motor.

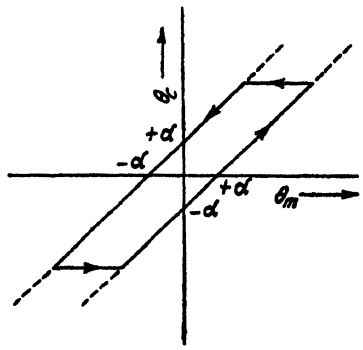

Fig. 2. Coupling unit characteristics.

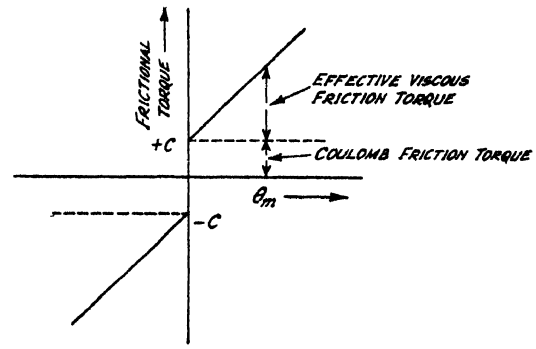

F.ig 3. Motor friction characteristics.

As has been derived in appendix I of part I the dynamics of the system in Fig. 1 is described by the following equations:

$$T_m\ddot{\theta}_m+\dot{\theta}_m+F = k\theta_e \qquad \ldots (1)$$

$$\theta_e = \theta_i-\theta_c \qquad \ldots (2)$$

where, θ_m—motor shaft position
θ_i—input shaft position
θ_c—output shaft position
T_m—motor time constant
F—coulomb friction torque,
and K—a constant, being the velocity-constant of the system that results if the nonlinearities in Fig. 1 are neglected.

The backlash characteristics shown in Fig. 2 relates the motor shaft position θ_m and the load shaft position θ_c and can be represented mathematically as

$$\left.\begin{aligned} \theta_c &= \theta_m - \alpha \frac{\dot{\theta}_c}{|\dot{\theta}_c|}; \ \dot{\theta}_c \neq 0 \\ |\theta_m - \theta_c| &< \alpha; \ \dot{\theta}_c = 0 \end{aligned}\right\} \quad \ldots (3)$$

α being the backlash half width.

And, the coulomb friction torque F is given by

$$\left.\begin{aligned} F &= C \frac{\dot{\theta}_m}{|\dot{\theta}_m|} \ ; \ \dot{\theta}_m \neq 0 \\ -C < F &< C \ ; \ \dot{\theta}_m = 0 \end{aligned}\right\} \quad \ldots (4)$$

C being the coulomb friction torque constant.

Eqs. (1) to (4) completely describe the system in Fig. 1.

SYSTEM TRANSIENT RESPONSE FROM FREQENCY RESPONSE DATA

(a) *General*

If the nonlinearities in Fig. 1 are assumed absent the time response of the system has definite correlationships with its frequency response. In presence of the nonlinearities there is of course no basis for such correlationship (the superposition principle being no longer valid). However, in the describing function method the nonlinearity is replaced by a slowly varying quasi-linear transfer function and it is still possible to obtain the transient response from the frequency response data, though such deductions are necessarily of approximate nature (Kochenburger 1950 and 1953). For this purpose the system in Fig. 1 is represented in the block diagram form in Fig. 4. The block $G_c(\theta_m)$ represents the describing function of the coulomb friction device and is given by (Hass 1953)

$$G_c(\theta_m) = \frac{4C}{\pi} \frac{1}{|\dot{\theta}_m|} \quad \ldots (5)$$

The block $G_B(\theta_m)$ represents the describing function of the coupling unit having backlash and is given by (Nichols 1953)

$$G_B(\theta_m) = [\beta^2+\gamma^2]^{\frac{1}{2}} \; ; \; \underline{/-\tan^{-1}(\gamma/\beta)} \qquad \ldots \quad (6)$$

$$\beta = \frac{1}{\pi}\,[\cos^{-1}(2n-1)+2(1-2n)\sqrt{n(1-n)}] \qquad \ldots \quad (7)$$

and

$$\gamma = \frac{4}{\pi}\,n(1-n) \qquad \ldots \quad (8)$$

where $n = \alpha/\hat{\theta}_m$, the normalised blacklash width.

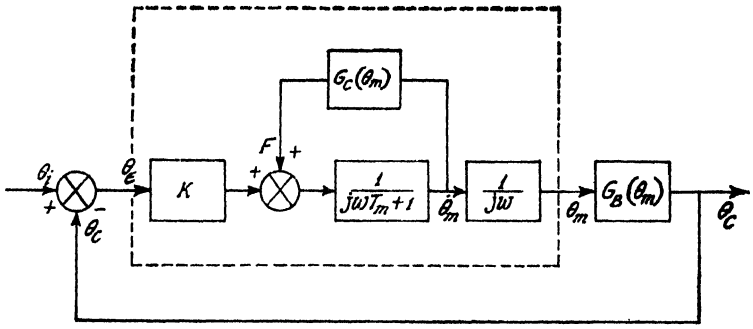

Fig. 4. Frequency response representation of the system.

The frequency response transfer function of the portion in Fig. 4 shown within the dotted box representing the motor with the coulomb friction is easily seen to be given by

$$G(j\omega, \theta_m) = \frac{K}{j\omega(j\omega T_m+1)+j\,\frac{4B}{\pi}} \; ; \qquad \ldots \quad (9)$$

$$B = \frac{C}{\hat{\theta}_m} \qquad \ldots \quad (10)$$

The total forward-loop transference of the system is then

$$\frac{\theta_C}{\theta_\varepsilon}\,(j\omega,\ \theta_m) = G(j\omega, \theta_m)\times G_B(\theta_m) \; ; \qquad \ldots \quad (11)$$

and the closed-loop transference is accordingly,

$$\frac{\theta_C}{\theta_i}\,(j\omega, \theta_m) = \frac{G_B(\theta_m)}{G(j\omega, \theta_m)^{-1}+G_B(\theta_m)} \qquad \ldots \quad (12)$$

The right-hand side of Eq. (12) incorporates the effects of the nonlinearities on the system frequency response. This is clearly dependent on both amplitude and frequency of the input signal. It is most convenient to assume the input signal to be a periodic function of time such that $\theta_m(t)$ varies sinusoidally i.e. $\theta_m(t) = \hat{\theta}_m \sin \omega t$. Then, using Eqs. (6) to (10) and Eq. (12) the closed-loop transfer function can be computed as a function of the frequency for a number of assumed values of the amplitude $\hat{\theta}_m$. These computations are conveniently carried out graphically in the manner outlined below:

The describing function - $G_B(\theta_m)$. is plotted in the complex plane as an amplitude locus. On the same plane are superposed plots of the frequency loci of $G(j\omega, \theta_m)^{-1}$ each locus being drawn for a specific value of $\hat{\theta}_m$. In Fig. 5 are shown these plots for the system in Fig. 4 for the assumed values of $K = 10$ and $T_m = 1$, using the normalised signal parameters n and B.

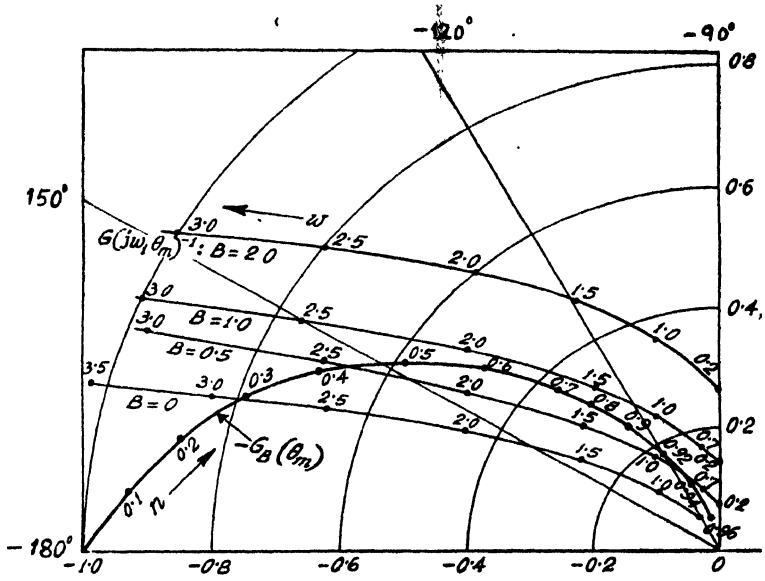

Fig. 5. Plots of $G(j\omega, \theta_m)^{-1}$ and $-G_B(\theta_m)$ in the complex plain.

Let us assume that the frequency response of the system corresponding to a signal amplitude $\hat{\theta}_m = \hat{\theta}_{m1}$ is desired. This is easily done by locating the point $G_B(\theta_{m1})$ on the amplitude locus (marked P in Fig. 5) and considering the frequency locus $G(j\omega, \theta_{m1})^{-1}$. Then at any frequency ω_1 (corresponding to the point Q in Fig. 5) the frequency response modulus is given by the ratio

$$\left| \frac{\theta}{\theta_i} \right|_{\substack{\hat{\theta}_m = \hat{\theta}_{m1} \\ \omega = \omega_1}} = \left| \frac{OP}{PQ} \right| \qquad \ldots \quad (13)$$

This ratio, if evaluated for a number of frequencies over the range of interest gives, when plotted against the frequency, the system frequency response corresponding to the signal amplitude $\hat{\theta}_m = \hat{\theta}_{m1}$. If this whole procedure is repeated for a number of values of $\hat{\theta}_m$ the frequency response of the system is evaluated as a function of amplitude and frequency. This can be done for different amounts of coulomb friction.

In Figs. 6(a), (b) and (c) are shown the frequency response curves of the system in Fig. 4 as obtained from the loci of Fig. 5 for three different cases corresponding

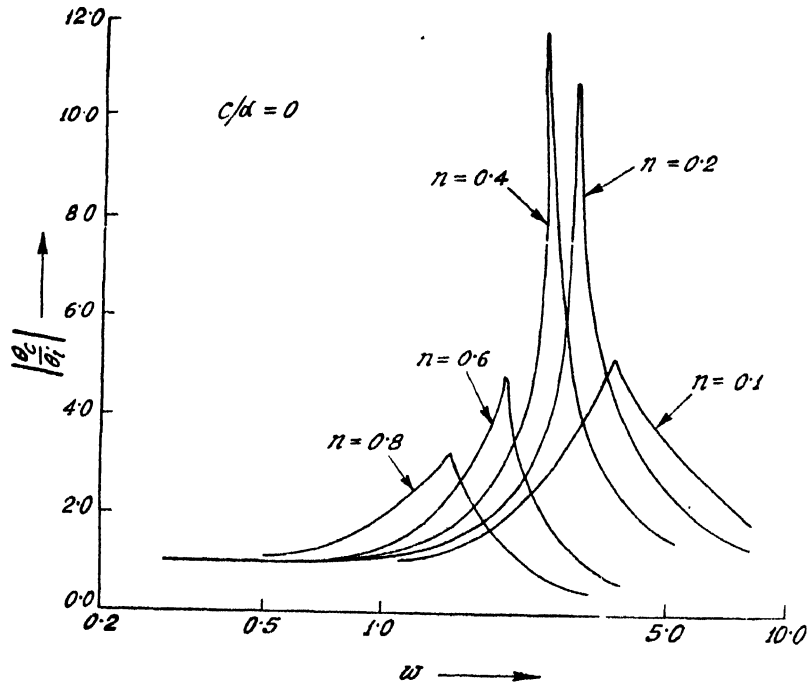

Fig. 6. (a) Frequency response plots : $C/\alpha = 0$

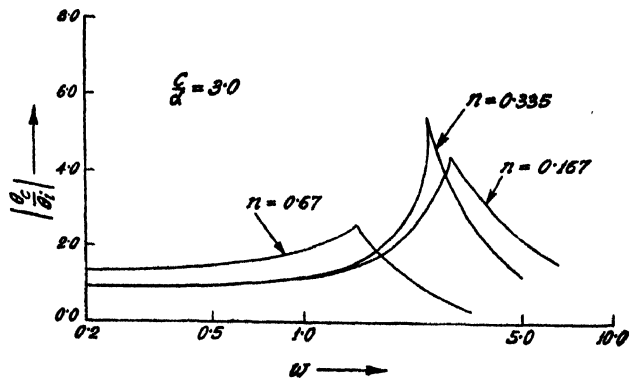

Fig. 6(b) $C/\alpha = 3.0$

to $C/\alpha = 0$, 3.0 and 5.0. The peak value of the ratio $|\theta_C/\theta_i|$ gives a measure of the system's relative stability and the frequency ω_r at which this peak occurs gives a measure of the system's speed of response.

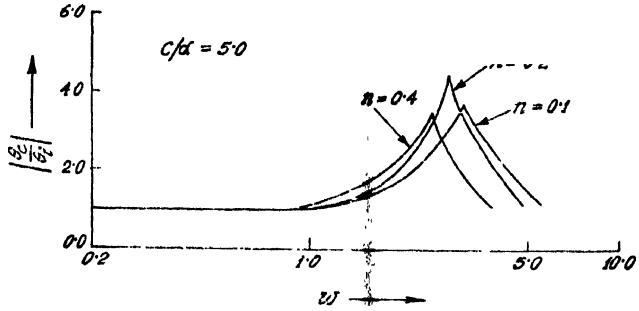

Fig. 6(c) $C/\alpha = 5.0$

(b) *Effects of the nonlinearities*

The effects of the two nonlinearities viz. backlash and coulomb friction, on the degree of stability as well as the speed of the response of the system can be seen from the frequency response curves of Fig. 6. In order to bring out the effects of the coulomb friction we proceed as follows :

Let us first assume that the motor is characterised by a truly linear friction characteristics so that instead of the quasilinear describing function $G(j\omega, \theta_m)$ given by Eq. (9) the motor is characterised by linear transfer function

$$G(j\omega) = \frac{K}{j\omega(j\omega T_m + 1)} \tag{14}$$

The resultant frequency response curves are shown in Fig. 6(a). These curves incorporate the effects of backlash alone. The values of $|\theta_C/\theta_i|'(\theta_m)$ and $\omega_r(\theta_m)$ obtained from these curves are plotted against the normalised amplitude n in Figs. 7(a) and (b) respectively (curves marked $C/\alpha = 0$). It is seen that the magnitude of the ratio $|\theta_o/\theta_i|$ increases with falling signal amplitude (i.e. with n increasing) until it reches an infinitely large value (at a signal amplitude corresponding to $n = .3$ in Fig. 8). This indicates a possibility of sustained oscillation (of this amplitude) in the system. The reduction of the magnitude of the response amplitude at still smaller values of the signal amplitude is of course to be expected since the effective gain approaches zero due to the backlash dead-zone. The region of instability (round about the signal amplitude of about 3.3 in the present case) is of the order of backlash width. It can be concluded therefore that the presence of backlash causes the system stability to be impaired primarily at comparatively small signal levels. Also there is a slight reduction in the values of $\omega_r(\theta_m)$ at smaller signal amplitudes thus reducing the system's speed of response.

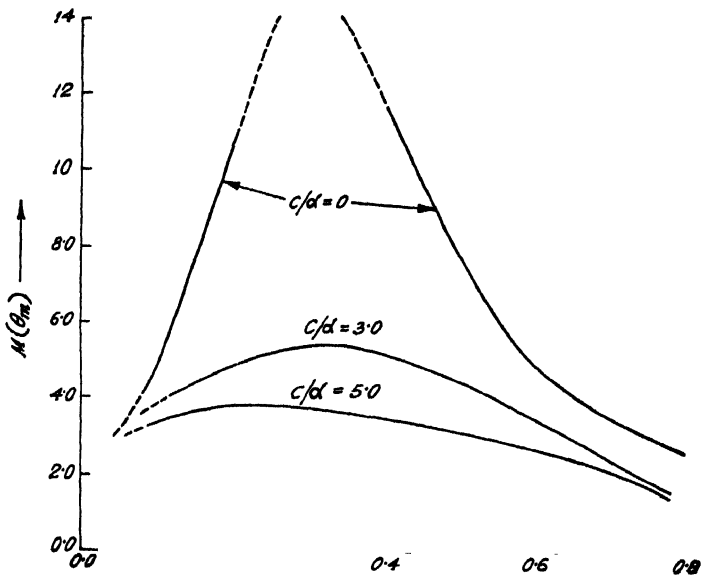

Fig. 7. Plots of (a) frequency-response peak $M(\theta m)$

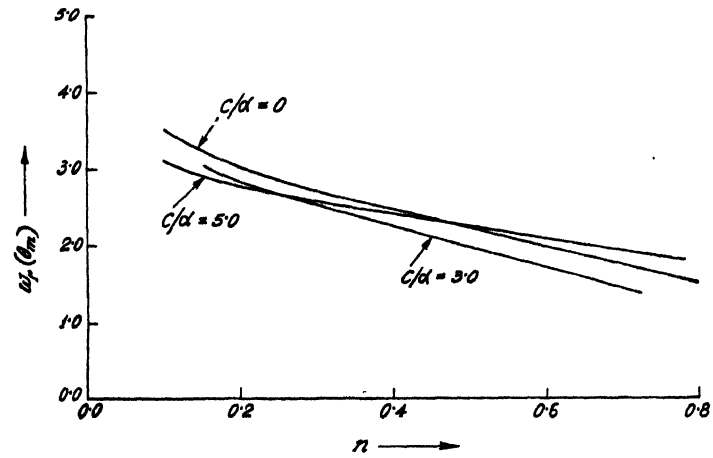

Fig. 7(b). frequency of occurrence of the peak $\omega_r(\theta m)$ against n.

If now the same parameters $|\theta_e/\theta_i|(\theta_m)$ and $\omega_r(\theta_m)$ are evaluated from the response curves of Figs. 6(b) and (c) the results of addition of the coulomb friction becomes evident. These also are plotted in Fig. 7 against n (curves marked $C/\alpha = 3.0$ and $C/\alpha = 5.0$) in order to emphasize the effects of the coulomb friction. It is seen that for the conditions specified the value of the frequency response peak as also the frequency show much less dependence on the signal amplitude; not only are the sustained oscillations avoided but addition of adequate coulomb friction can effectively improve the system's damping at small signal levels.

These results are in fact to be expected from the form of the describing function $G(j\omega, \theta_m)$ as given by Eq. (9). It is seen that the effect of considering only the fundamental component of the coulomb friction torque for an assumed sinusoidal motor speed is to replace the nonlinear friction by an equivalent amplitude-dependent viscous friction $4C/\pi|\dot{\theta}_m|$, a quantity which is predominent at comparatively smaller values of $\hat{\theta}_m$.

TIME RESPONSE FROM THE SOLUTION OF THE CHARACTERISTIC EQUATIONS

The discussions in the previous sections give a qualitative picture of the effects of coulomb friction on the stability and the speed of the response of a servo system having backlash in the output coupling. A more quantitative analysis of the problem is, however, possible by following a method suggested by Oldenburg and Sartorius (1948). This consists of solving certain piecewise linear differential equations which characterise the system under the stipulated conditions. To set up these equations we start with a typical step response of a system which has low damping. This is indicated in Fig. 8; a response which exhibits some oscillations before attaining the steady state value. Taking $t = 0$ at the instant at which

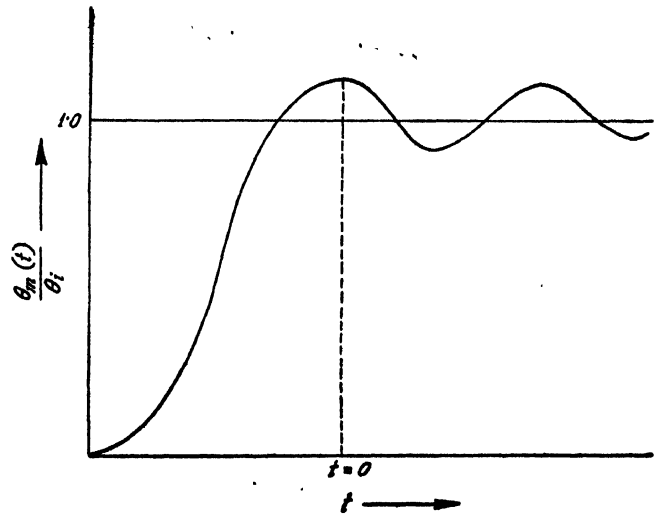

Fig. 8. A typical step input response of the system.

the first overshoot occurs the function $\theta_m(t)$ in Fig. 8 can be considered as a damped sinusoid, at least during the first few oscillations. The relationship between the motor shaft and outputshaft positions can then be set up as

$$\left.\begin{aligned} \theta_o &= \hat{\theta}_{m0} - \alpha; \quad 0 \leqslant \omega t \leqslant \theta_2 \\ &= \theta_m + \alpha; \quad \theta_2 \leqslant \omega t \leqslant \pi \end{aligned}\right\} \qquad \ldots (15)$$

where $\hat{\theta}_{m0}$ = the initial amplitude of oscillation
and $\theta_2 = \cos^{-1}(1-2\alpha/\hat{\theta}_{m0})$ } ... (16)

These quantities are defined as in Fig. 9. Now substituting for θ_c in Eq. (1) and setting $\theta_i = 0$ we get the two following equations which are valid for the two sections of the half period of $\theta_m(t)$ defined in Eq. (15). Thus, for

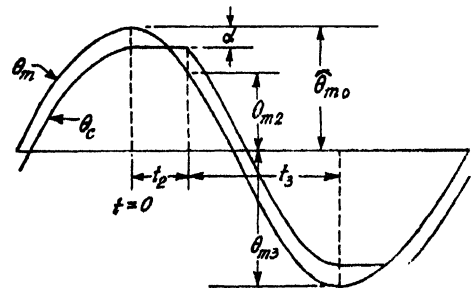

FIG. 9. Waveforms illustrating the boundary conditions.

$$0 \leqslant t \leqslant \theta_2/\omega,$$

$$T_m \frac{d^2\theta_m}{dt^2} + \frac{d\theta_m}{dt} = C - K(\hat{\theta}_{m0} - \alpha) \qquad \ldots (17)$$

the boundary conditions being

$$t = 0, \qquad \theta_m = \hat{\theta}_{m0} \quad \text{and} \quad \dot{\theta}_m = 0$$

and $t = t_2(\text{say}) = \theta_2/\omega, \quad \theta_m = \hat{\theta}_{m0} - 2\alpha = \theta_{m2}$ (say)

and $\dot{\theta}_m = [\dot{\theta}_m]_2$ (say), which is a negative quantity.

For the other section using a new independent variable t_1 i.e. for

$$0 \leqslant t_1 \leqslant \theta_3/\omega \text{ (say)},$$

$$T_m \frac{d^2\theta_m}{dt_1^2} + \frac{d\theta_m}{dt_1} + K\theta_m = C - K\alpha \qquad \ldots (18)$$

—the boundary conditions being

$t_1 = 0, \quad \theta_m = \theta_{m2}$ and $\dot{\theta}_m = [\dot{\theta}_m]_2$, as obtained from the previous section,

and $t_1 = t_3 = \theta_3/\omega, \qquad \theta_m = \theta_{m3}$(say) and $\dot{\theta}_m = 0$.

Eqs. (17) and (18), subject to the specified boundary conditions, can now be solved to give the nature of the system response during the half period in question. The solution can then be used to compute such transient response parameters as the half period decrement and the half period of the transient oscillations. The results of these computations involve the nonlinearities and bring out their effects on the system response. In terms of the symbols used above these two parameters require evaluation of θ_{m3} and (t_2+t_3). The procedure for the purpose is outlined below :

Solution of Eq. (17) gives

$$\theta_m(t) = \hat{\theta}_{m0} - k(t - T_m + T_m e^{-t/T_m}) \qquad \ldots (19)$$

where
$$k = K(\hat{\theta}_{m0} - \alpha) - C \qquad \ldots (20)$$

Substituting $t = t_2 = \theta_2/\omega$,

$$\theta_{m2} = \hat{\theta}_{m0} - 2\alpha = \hat{\theta}_{m0} - k(t_2 - T_m D) \qquad \ldots (21)$$

where
$$D = 1 - e^{-t_2/T_m} \qquad \ldots (22)$$

Eqs. (21) and (22), when solved, gives t_2.

Solution of Eq. (18) gives

$$\theta_m(t_1) = \frac{C}{K} - \alpha + \left(\alpha - \frac{C}{K} + \theta_{m2}\right) e^{-\rho t_1} \cos \lambda t_1$$

$$+ \frac{1}{\lambda}\left[\rho\left(\alpha - \frac{C}{K} + \theta_{m2}\right)\right] e^{-\rho t_1} \sin \lambda t_1 \qquad \ldots (23)$$

where ρ and λ are two parameters given by

$$\rho = \frac{1}{2T_m} \; ; \quad \rho^2 + \lambda^2 = K/T_m \qquad \ldots (24)$$

Substitution of the terminating condition in (23) leads to

$$\tan \lambda t_3 = \frac{\lambda D/\rho}{D-2} \qquad \ldots (25)$$

This gives t_3.

Also putting $t_1 = t_3$ in (23) we get

$$\theta_{m3} = \frac{C}{K} - \alpha + \frac{\left(\hat{\theta}_{m0} - \alpha - \frac{C}{K}\right)(1 - D + D^2 K T_m)}{1 - D/2} e^{-\rho t_3} \cos \lambda t_3 \qquad \ldots (26)$$

From (26) we have

$$\frac{\theta_{m3}+\alpha}{\hat{\theta}_{m0}-\alpha} = \frac{C}{K(\hat{\theta}_{m0}-\alpha)} + \frac{\hat{\theta}_{m0}-\alpha-\frac{C}{K}}{\hat{\theta}_{m0}-\alpha} \cdot \frac{1-D+D^2KT_m}{1-D/2} \; e^{-\rho t_3} \cos \lambda t_3 \quad \ldots \quad (27)$$

Noting (Fig. 9) that θ_{m3} has a negative value, Eq. (27) can be rewritten as

$$\Delta = \frac{|\theta_{m3}|-\alpha}{\hat{\theta}_{m0}-\alpha} = \frac{\theta_{m0}-\alpha-\frac{C}{K}}{\hat{\theta}_{m0}-\alpha} \; \frac{1-D+D^2KT_m}{D/2-1} \; e^{-\rho t_3} \cos \lambda t_3$$

$$- \frac{C}{K(\hat{\theta}_{m0}-\alpha)}$$

$$= \left[1 - \frac{C/\alpha}{K(\phi_{m0}-1)}\right] H - \frac{C/\alpha}{K(\phi_{m0}-1)} \quad \ldots \quad (28)$$

where $\phi_{m0} = \hat{\theta}_{m0}/\alpha$—the normalised amplitude.

The left hand side of this equation is easily identified as the half period decrement of $\theta_O(t)$, the load motion. On the right hand side of (28) the factor H represents the half-period decrement of the load motion when the coulomb friction constant C is zero. This factor has been worked out by Nichols (1953) who studied the effects of backlash in a servo system. The effect of the coulomb friction is obviously to reduce this value thus indicating a stabilising action.

For given values of the system constants the half period decrement given by (28) and the half period given by $T/2 = t_2+t_3$ as obtained from Eqs. (21) and (22) and Eq. (25) respectively, can be computed. The results are plotted in Fig. 10 against the normalised signal amplitude $\phi_{m0}-1 = (\hat{\theta}_{m0}-\alpha)/\alpha$ using the normalised coulomb friction constant C/α as a parameter. The curves of Fig. 10 point out that the effects of the coulomb friction predominate when the signal amplitude is small. In general an increase in the value of C results in a reduction of Δ and slight increase of the half-period. The results are in agreement with the earlier conclusions of the qualitative discussions.

RESULTS OF SIMULATOR STUDIES

The arrangement of the simulator has been discussed in reference 1 and is shown in Fig. 11. The simulator is capable of varying the normalised coulomb friction constant C/α as well as the gain K. The response $\theta_m(t)$ for step displacement inputs under different conditions of gain and the constant C/α have been

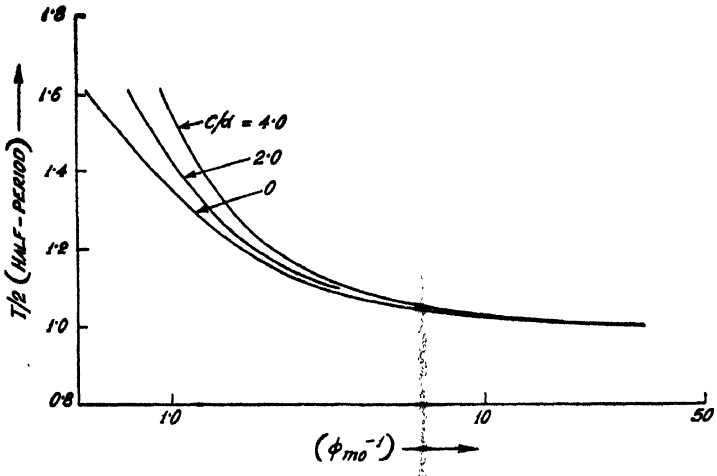

Fig. 10(a). Plots of the half-period decrement Δ against $\phi_{m_s}^{-1}$.

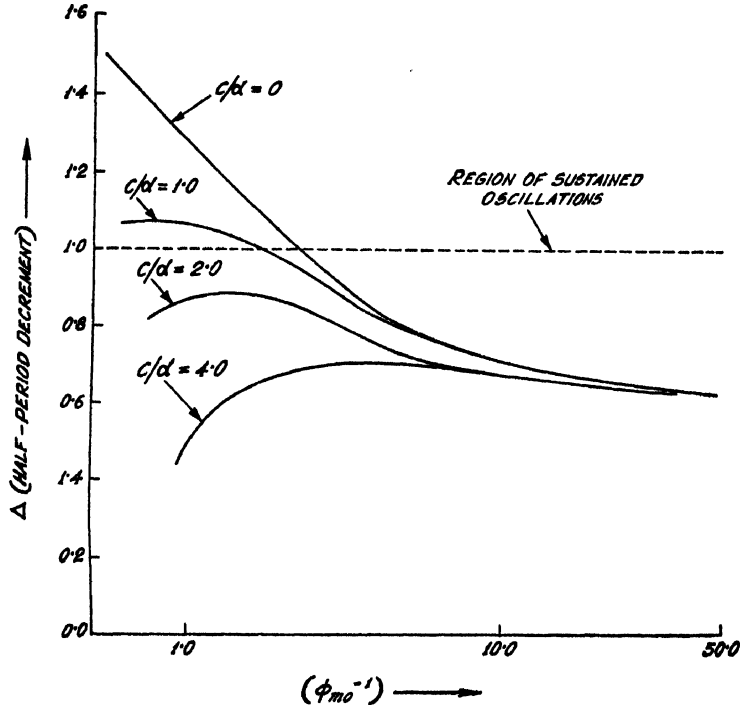

Fig. 10(b). Plots of half period T/2 against ϕ_{m0}^{-1}.

obtained and are displayed in the traces of Figs. 12(a) and (b). In Fig. 12(a) are shown traces of response for a gain $K = 4.0$ and $C/\alpha = 0$, 2.5 and 4.0. In Fig. 12(b) are shown traces of the response for $K = 2.0$ and $C/\alpha = 0$, 2.5 and 4.0. The stabilising actions of the columb friction are clearly displayed by these traces.

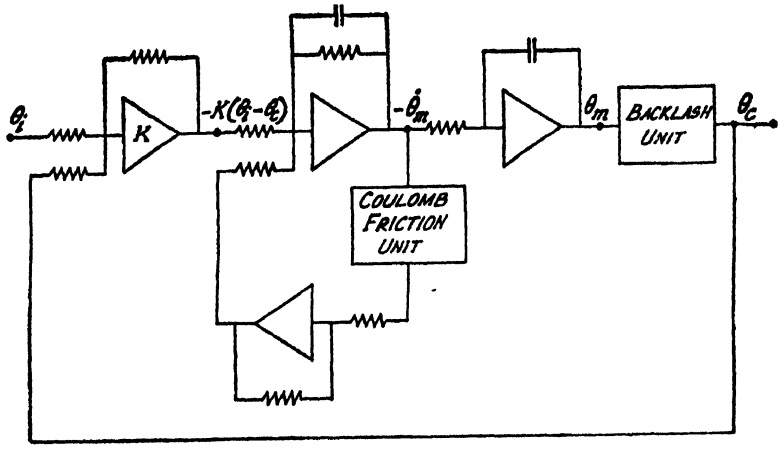

FIG. 11. Simulator set up for the system.

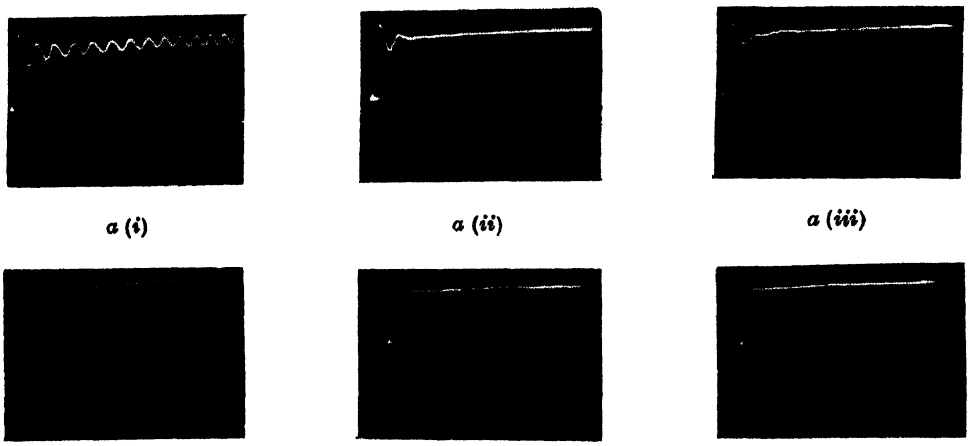

a (i) *a (ii)* *a (iii)*

b (i) *b (ii)* *b (iii)*

FIG. 12. Traces of step responses obtained with the help of the simulator:
(a) $K=4.0$; $C/\alpha=0$, 2.5 and 4.0
(b) $K=2.0$; $C/\alpha=0$, 2.5 and 4.0

CONCLUSIONS

The frequency response data indicate that the presence of coulomb friction in a servomechanism results in an increase of the effective system damping at relatively low signal amplitudes. If the servo system has backlash in the output coupling, coulomb friction can accordingly provide a proper compensation for the backlash effects. Solutions of the piece-wise linear differential equations which characterise the system having the two nonlinearities can be obtained to provide with quantitative data regarding the effects of the two nonlinearities on such transient response parameters as the half period decrement and the half period.

Conclusions drawn from these computations are corroborated by the results of analogue computer studies.

ACKNOWLEDGMENT

The author is greatful to Prof. J. N. Bhar for his guidance and to Dr. A. K. Choudhury for discussions. The award of a scholarship by the Government of India is also thankfully acknowledged.

REFERENCES

Haas, V. B., 1953, *Trans. A. I. E. E.*, **72**, Part 2, pp. 119-123.
Kochenburger, R. J., 1950, *Trans. A.I.E.E.*, **69**, Part 1, 270.
Kochenburger, R. J., 1953, *Trans. A.I.E.E.* **72**, Part 2, 180.
Mahalanobis, A. K., 1960, A.I.E.E. paper No. DP 60-667.
Nichols, N. B., 1953, *Trans. A.I.E.E.*, **72**, Part 2, 482.
Oldenbourg, R. C. and Sartorius, H., 1948, Dynamics of Automatic Controls (book), Transaction by A.S.M.E., New York, N.Y., pp. 168-173.